Hydrogen Bonding Competition Mediated Phase Separation with Abnormal Moisture-Induced Stiffness Boosting

Jian Xu, Baohu Wu, Lei Hou, and Peiyi Wu**

Moisture usually deteriorates polymers' mechanical performance owing to its plasticizing effect, causing side effects in their practical load-bearing applications. Herein, a simple binary ionogel consisting of an amphiphilic polymer network and a hydrophobic ionic liquid (IL) is developed with remarkable stiffening effect after moisture absorption, demonstrating a complete contrast to water-induced softening effect of most polymer materials. Such a moisture-induced stiffening behavior is induced by phase separation after hydration of this binary ionogel. Specifically, it is revealed that hydrogen (H)-bonding structures play a dominant role in the humidity-responsive behavior of the ionogel, where water will preferentially interact with polymer chains through H-bonding and break the polymer-IL H-bonds, thus leading to phase separation structures with modulus boosting. This work may provide a facile and effective molecular engineering route to construct mechanically adaptive polymers with water-induced dramatic stiffening for diverse applications.

1. Introduction

Stiffness-switching presents a critical strategy for organisms in nature to accommodate complicated living conditions. For instance, fish can change its skin modulus under external stimuli to minimize surface friction force and escape from dangerous situations.[1] Sea cucumber shares the talent of rapid and reversible altering its tissue stiffness either to prevent physical damage or move freely.[2] Inspired from nature, synthetic polymer materials, which can change stiffness on-demand, provide a dynamic solution with simultaneous shape adaptability and load-bearing capability, showing great potentials in modern society for diverse applications, including intelligent electronics, soft robots, artificial muscles, reversible adhesives, etc.[3] Currently, a series of smart polymer materials with mechanical adaption have been developed through introducing stimuli-induced glass transition,[4] crystallization-melting transition[5] and phase separation.[6] Herein, the triggers to induce the stiffness-switching include heat, light, solvents or electricity. Among them, water is an abundant yet renewable resource and poses no risks to the environment, offering a low-carbon stimulus to be operated in mild conditions. Nevertheless, water usually acts as a plasticizer and weakens the molecular interactions between polymer chains,[7] resulting in the deterioration of polymer's mechanical performance and consequently hindering their load-bearing applications at high humidity.

Currently, many efforts have been devoted to overcoming the water-induced softening of common polymer systems, including water-mediated hydrogen bonding,[8] hydration-triggered chemical reaction,[9] water-induced phase separation[9b,10] etc. Phase separation may result in the decomposition of polymer gels into dense and sparse polymer regions in real space, yielding associated polymer chains in the dense phase and thereby producing boosted stiffness. Thus, it is indicated that phase separation would be an efficient way to achieve water-induced enormous stiffness increasing of polymer materials. Wooley et al.[11] demonstrated that an amphiphilic crosslinked polymer, composed of hyperbranched fluoropolymer and poly(ethylene glycol) (PEG), exhibits an increase in elastic modulus upon absorbing water. Tan et al.[12] reported water-triggered stiffening of shape-memory polyurethane, which features hard segments on the main chains and soft PEG segments on the side chains, through enhanced microphase separation. Recently, Zhu et al.[13] designed a series of three-component polymer gels, consisting of a hydrophobic poly(benzyl methacrylate) network, a hydrophobic ionic liquid (IL) and a hygroscopic salt, with dramatic mechanical stiffening in virtue of water-driven phase separation. However, these strategies either show limited modulus change amplitudes or require complicated molecular design and delicate formulation optimization, which might restrict the practical applications.

Molecular interactions play a crucial role in the plasticizing effect of water on polymer materials owing to the strong capability of water to form hydrogen (H) bonds with polymer chains. From this point of view, we hypothesize that water molecules could participate in the H-bonding competition in a binary gel

J. Xu, L. Hou, P. Wu
State Key Laboratory for Modification of Chemical Fibers and Polymer Materials
College of Chemistry and Chemical Engineering
Donghua University
Shanghai 201620, China
E-mail: houlei@dhu.edu.cn; wupeiyi@dhu.edu.cn
B. Wu
Jülich Centre for Neutron Science (JCNS) at Heinz Maier-Leibnitz Zentrum (MLZ) Forschungszentrum Jülich
Lichtenbergstr. 1, 85748 Garching, Germany

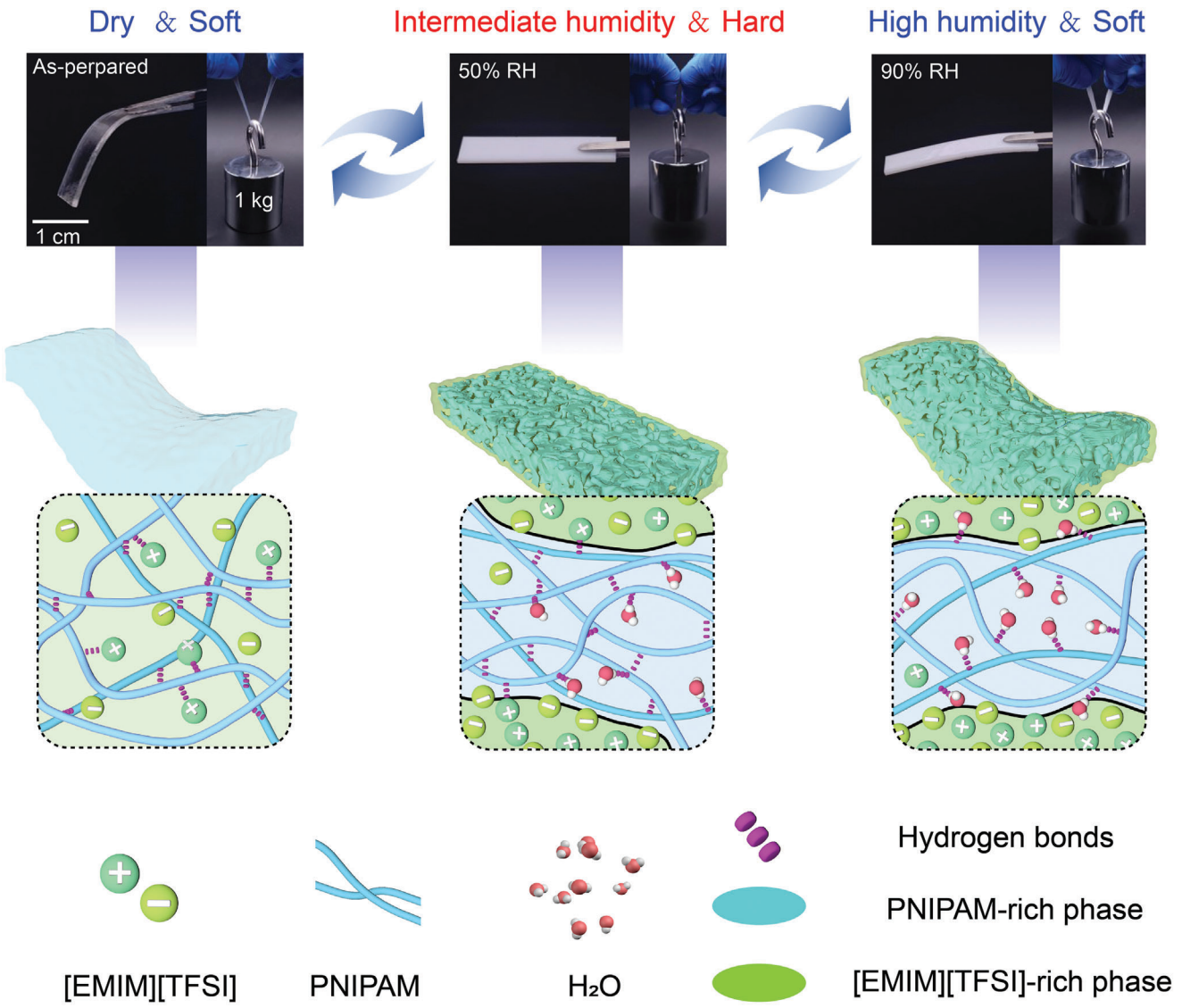

Figure 1. Photographs and schematic illustration of water-induced phase separation and stiffening of the PNIPAM/[EMIM][TFSI] ionogel.

system, which contains an amphiphilic polymer network and a hydrophobic solvent with modest compatibility, and subsequently induce phase separation to realize dramatic modulus increase. Poly(*N*-isopropylacrylamide) (PNIPAM) displays an upper critical solution temperature (UCST) in a hydrophobic IL,[14] e.g. ethyl methyl imidazolium bis (trifluoromethylsulfonyl) imide ([EMIM][TFSI]), suggesting that polymer–polymer and polymer–solvent interactions are subtle in this system. In addition, PNIPAM chains possess both hydrophilic and hydrophobic groups and can form H bonds with water molecules. Thus, in this work, we fabricate a binary PNIPAM/[EMIM][TFSI] ionogel as a model to test our hypothesis. As expected, the binary ionogel with proper polymer contents transforms from a transparent and soft state into an opaque and highly stiff one after moisture absorption, which is highly reversible. It is demonstrated that water could interact with PNIPAM chains through H-bonding and break the PNIPAM-IL H bonds, leading to phase separation structures with IL-rich and IL-poor phases and subsequent modulus boosting. The current work may provide a paradigm to develop mechanically adaptive materials with water-induced dramatic stiffening for diverse applications.

2. Results and Discussion

2.1. Effect of Moisture Absorption on the Mechanical Performance

The binary ionogels were facilely prepared by free radical polymerization of N-isopropylacrylamide in [EMIM][TFSI] in the presence of chemical cross-linker. As shown in **Figure 1**, the as-prepared ionogel is in a transparent and soft state, and could hardly bear its own weight. Meanwhile, it transforms into a white and rigid state after moisture absorption, and could lift a weight of 1 kg with a strip size of 30 mm (length) × 8 mm (width) × 1 mm (thickness), demonstrating the water-induced phase

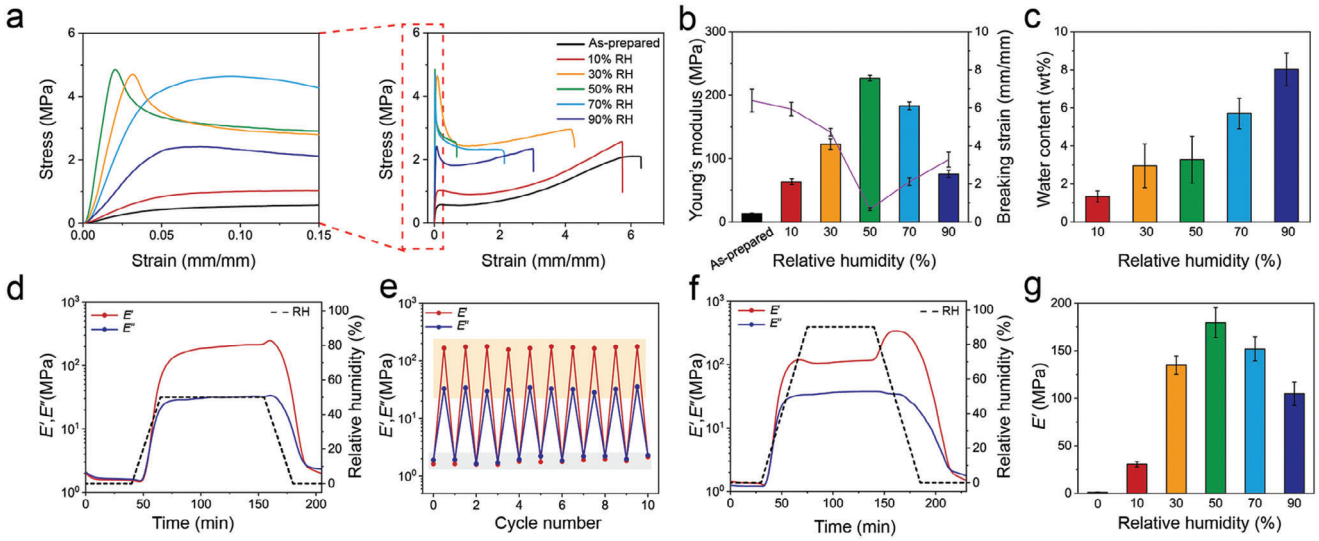

Figure 2. Humidity-induced mechanical performance variation of PNIPAM/[EMIM][TFSI] binary ionogel: tensile stress–strain curves a), Young's modulus and breaking strain b) and water content c) at varied RH. DMA curves d) and corresponding cycling tests e) of *E'* and *E''* with varying RH between 0 and 50%. f) DMA curves of *E'* and *E''* with varying RH between 0 and 90%. g) *E'* at varied RH.

separation and subsequent stiffening process. It is noted that the binary ionogel become soft again after further water absorption. We believed that H-bonding competition in the ionogel plays a crucial role for the non-monotonic change in stiffness with relative humidity (RH) increasing. In the dry state, the delicate balance between polymer-polymer and polymer-IL H-bonding could afford a homogeneous and soft binary ionogel. Water possesses a strong tendency to form H bonds with polymer chains and will compete with IL, leading to the disruption of polymer-IL H bonds and consequently microphase separated structure. Such a phase separation would bring polymer chains closer and lead to associated chains in the dense polymer phase, thereby leading to increased stiffness. Through further hydration, water molecules will continue to interact with polymer chains and subsequently break polymer–polymer H bonds, acting as a plasticizer to soften the ionogel.

We first examine the effect of polymer concentration on the water-responsive behavior of the binary ionogels. As displayed in Figure S1 (Supporting Information), the as-prepared ionogels show a nontransparent appearance at relatively low polymer fractions, while they are transparent at polymer concentrations higher than 30 wt%, which is consistent with the UCST-type phase behavior of PNIPAM in [EMIM][TFSI] determined by the composition dependence of the entropy and energy changes on mixing. It is observed that all the samples exhibit a stiffening behavior after moisture absorption at 50% RH owing to the water-induced/enhanced phase separation. As shown in Figure S2 (Supporting Information), the cloud points of the ionogels increase notably after water absorption. Herein, the sample of 30 wt% polymer content demonstrates an obvious phase separation with large modulus change, which will be chosen for further investigations. In the following part, the polymer content is 30 wt% unless otherwise specified.

Then, the mechanical performance of the ionogel at varied RH was evaluated through a universal tensile test. As shown in **Figure 2**a,b, the as-prepared ionogel is soft and stretchable with Young's Modulus (*E*) of 13.3 MPa and breaking strain (ε_b) of 640%. After moisture absorption, an obvious stiffening behavior could be observed. With RH varying from 0 to 90%, *E* of the ionogel first increases remarkably from 13.3 to 226.8 MPa and then decreases to 75.9 MPa. In contrast, ε_b of the ionogel exhibits a sharp decrease from 640% to 67%, followed by an increase to 330%. It is noticed that the ionogel displays a maximum *E* of 226.8 MPa, a minimum ε_b of 67% and toughness of 2.1 MJ m^{-3} (Figure S3, Supporting Information) at 50% RH, possibly due to the dense phase separation. Water content is critical in determining the mechanical properties of the ionogel. As expected, higher RH leads to higher water content, which could be as high as 8 wt% for the ionogel equilibrated at 90% RH (Figure 2c). From this point of view, a proper amount of water in the ionogel contributes to the phase separation with boosted modulus, whereas additional hydration of the ionogel causes plasticizing effect and deteriorates the stiffness (Figure S4, Supporting Information).

Dynamic mechanical analysis (DMA) was further performed to in situ monitor the mechanical change of the ionogel under various RH, as shown in Figure 2d. With increasing the RH from 0% to 50%, the storage modulus (*E'*) and loss modulus (*E''*) demonstrate a sharp increase from 1.3 to 179.6 MPa and 1.4 to 34.2 MPa, respectively. Herein, the slight decrease in modulus when equilibrated at 0% RH might be originated from trace amount of water in the as-prepared ionogel. Meanwhile, both *E'* and *E''* can return to the original values after RH decreasing to 0%, indicating that the stiffness-switching of the ionogel is highly reversible. Such a complete reversibility can be also confirmed by the excellent cycling performances of *E'* and *E''* under repeated RH switching between 0 and 50% (Figure 2e; Figure S5, Supporting Information). When increasing the RH from 0 to 90%, *E'* of the ionogel first increases dramatically and then decrease gradually, suggesting a highest modulus at intermediate humidity. It is noted that decreasing the RH from 90% to 0% affords higher modulus in the intermediate RH when compared with the RH

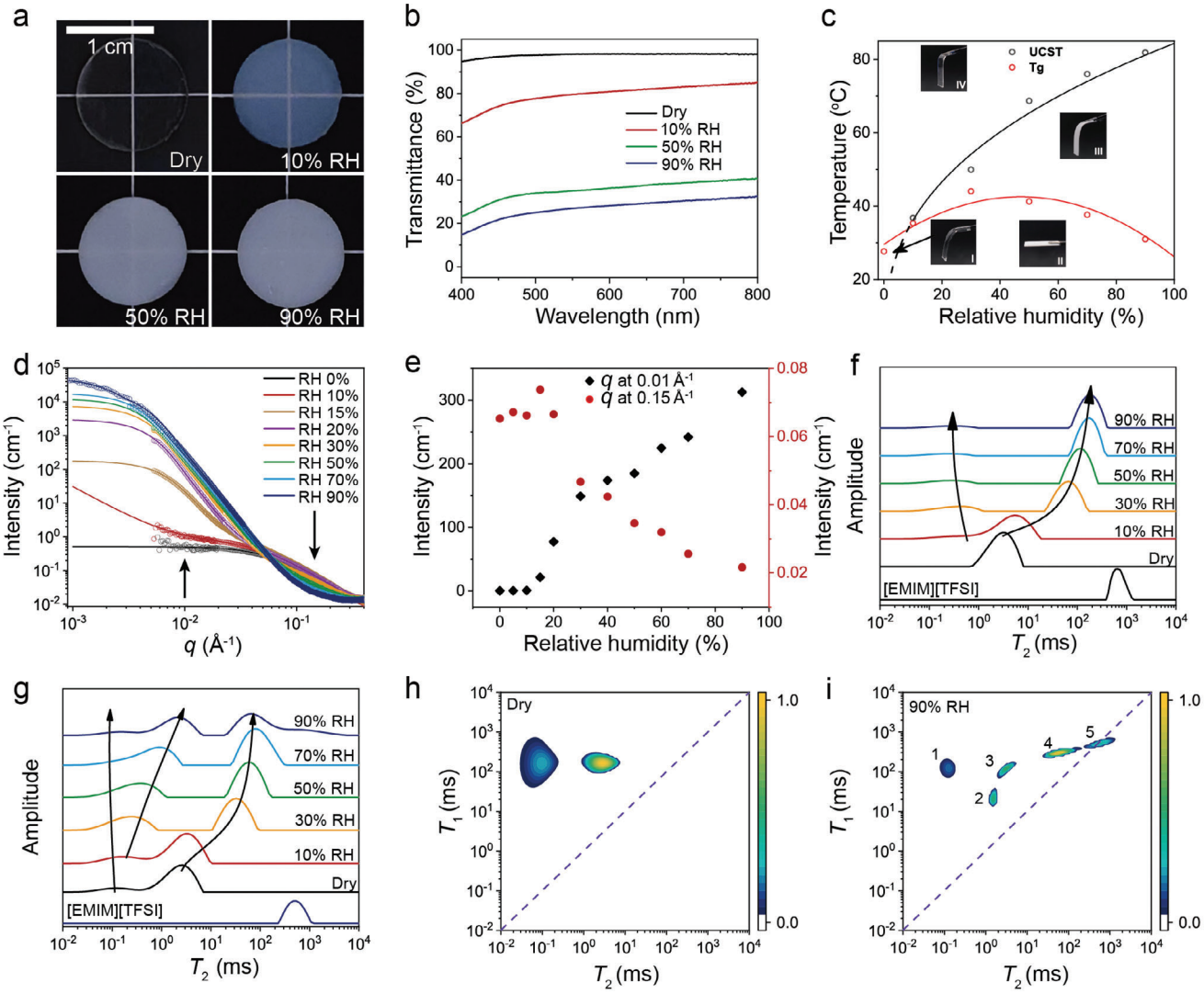

Figure 3. Water-induced phase separation of the PNIPAM/[EMIM][TFSI] binary ionogel: a) Photographs and b) transmittance of the ionogel in the dry state and equilibrated at different RH. c) UCST and T_g curves against RH. Humidity-dependent d) SAXS-USAXS profiles in logarithmic scales and e) scattering intensity at $q = 0.01$ and 0.15 Å^{-1}. LF ^{19}F NMR f) and LF ^{1}H NMR g) spectra at varied RH. h,i) 2D LF ^{1}H NMR spectra at varied RH.

increasing process, which might be explained by that decreasing the RH would first lead to the desorption of weakly bonded water molecules and this part of molecules acts merely as plasticizer. Figure 2g and Figure S6 (Supporting Information) displays the E' values of the ionogel equilibrated at different RH and reveals that 50% RH results in the most prominent stiffening, which parallels with the data from tensile tests.

2.2. Water-Induced Phase Separation

Phase separation plays a predominant role in the water-induced stiffening behavior of PNIPAM/[EMIM][TFSI] ionogel. **Figure** 3a,b shows that the ionogel gradually transforms from a transparent state to a semi-transparent one and finally becomes opaque with RH increasing, implying a phase transition process thereinto. Considering the UCST-type transition of PNIPAM in [EMIM][TFSI], we believe that the presence of water would significantly influence the phase transition temperature of the binary ionogel. As displayed in Figures S7 and S8 (Supporting Information), the as-prepared ionogel remains transparent even after cooling to −60 °C while demonstrates a UCST-type transition of ≈70 °C when equilibrated at 50% RH. In addition to phase separation, glass transition would also lead to stiffness change for a polymer system. Glass transition temperatures (T_g) of the ionogel equilibrated at varied RH are determined from rheological measurement (Figure S9, Supporting Information). Herein, the UCST and T_g curves are plotted against RH in Figure 3c. It is shown that the ionogel is rigid only in the region with phase separation below T_g, indicating that the synergy between phase separation and glassy state of the ionogel contribute to the water-induced stiffening.

The phase separation in ionogels induced by humidity was further analyzed using in situ small-angle X-ray scattering (SAXS)

and ultra small-angle X-ray scattering (USAXS) methods, as shown in Figure 3d,e and Figures S10 and S11 (Supporting Information). The scattering contribution can be roughly divided into two regimes: the low q regime ($q < 0.02$ Å^{-1}), where the scattering dominated by the large separate phases; the high q regime ($q > 0.02$ Å^{-1}), where the scattering contributed mostly by the local structure of the polymer matrix. Scattering is roughly divided into 4 stages (T1–T4) according to the controlled humidity and a developing model is used to fit the data (Supporting Information theory part).

In the dry state (T1), the SAXS profile of the ionogel exhibits a typical homogeneous conventional polymer gel, which can be described by the Ornstein–Zernicke function.[15] From RH10% onward (T2), minor changes occur in the high q range, alongside a significant increase in scattering in the low q region. This suggests the presence of polymer chain interactions due to water molecules, resulting in a clustering effect within the dry film. At the T3 stage, scattering intensity in the low q region escalates rapidly starting from RH15%, while scattering in the high q range weakens (except for RH15%). This is attributed to polymer chain collapse, leading to phase separation. The scattering curve from RH15% to RH70% is well-described using a multi-component system model (see Supporting Information for details). Fitting results include calculated parameters such as the correlation length (ξ, or blob size) describing polymer chain behavior, radius of gyration (R_g), morphology-related parameter n, and forward scattering I_0. The calculated correlation length, ξ, shows a slight increase with humidity from 17.5 Å at RH0% to 25 Å at RH15%, indicating initial interactions between water molecules and polymer chain segments, increasing the average distance between chains. However, beyond RH15%, polymer chains gradually collapse, leading to phase separation. The correlation length initially decreases rapidly, plateauing before continuing to decrease to 8.7 Å at RH70%. This decrease in correlation length correlates with stiffening of the ionogel, consistent with other characterizations. The morphology parameter n, reflecting sample morphology, remains around 4 from RH15% and above, indicating a condensed phase with clear interface in the phase-separated system. The R_g ranges from 272 Å for RH15% to 484 Å for RH75%. Changes in R_g and forward scattering exhibit similar trends, indicating rapid increase in scattering intensity in the low q region mainly due to size growth of the new separated phase.

In the T4 stage, scattering exhibits a sudden upward turning point at 0.0006 Å on the Log–Log plot, indicating further interaction and cross-linking of the new phase under RH90% humidity. Scattering appears flat at high q under Log–Log scale, suggesting few discrete polymer phases in the system. Calculated $R_g > 600$ Å at RH90% is significantly larger than R_g at RH70%, indicating substantial deviation caused by mutually cross-linked separated phases. In summary, the SAXS-USAXS characterization results unequivocally demonstrate phase separation induced by the collapse of polymer chains in samples exposed to varying humidity levels, which correlates with their mechanical properties.

Low-field nuclear magnetic resonance (LF NMR), a powerful tool to probe the activity changes of certain atoms through transverse (spin–spin) relaxation times (T_2), is employed to gain molecular insights into the phase structures of the ionogel. First, LF ^{19}F NMR spectra (Figure 3f) are collected to monitor the behavior of [EMIM][TFSI]. For the dry ionogel, only one T_2 peak is observed, hinting the homogeneous distribution of [EMIM][TFSI] in the ionogel. With RH increasing, the T_2 peak broadens and then splits into two peaks, suggesting the phase transition of the ionogel into two phases after moisture absorption. Herein, the lower T_2 peak with only a small portion represents [EMIM][TFSI] confined in the PNIPAM-rich phase while the higher one represents [EMIM][TFSI] in the PNIPAM-poor phase. Furthermore, LF ^{1}H NMR spectra are obtained to recognize all the proton species in the ionogel. As shown in Figure 3g, two peaks could be identified from the ionogel in the dry state, which could be related to protons in PNIPAM and [EMIM][TFSI] from low to high T_2, respectively. After hydration, the occurrence of phase separation results in the formation of polymer-rich and polymer-poor phases. At intermediate RH, protons in the polymer-rich phase, which mainly come from PNIPAM and water, are strongly confined and bonded, thus demonstrating low T_2. Meanwhile, protons in the polymer-poor phase are mostly contributed by [EMIM][TFSI] and less restricted, consequently showing relatively high T_2. Further increasing the RH to 90% distinguishes two species in the polymer-rich phase, which could be assigned to PNIPAM and water from low to high T_2, respectively, suggesting that water molecules are tightly bonded in the polymer-rich phase at intermediate RH while show increased mobility at high RH. It is noticed that the T_2 of both ^{19}F and ^{1}H changes significantly from 10% to 30% RH, indicating that the phase transition occurs evidently in this RH region, which parallels with the SAXS-USAXS results as well as the modulus change in Figure 2g. 2D LF-^{1}H NMR T_1-T_2 spectra, where T_1 represents longitudinal (spin-lattice) relaxation time, are obtained to provide more precise information on the proton species in the ionogel (Figure 3h,i; Figure S12, Supporting Information). Generally, a higher T_1/T_2 ratio indicates a lower mobility and the diagonal line with $T_1/T_2 = 1$ donates a highly mobile liquid in the bulk state.[16] It is noteworthy that five populations can be observed in the ionogel after moisture absorption at 90% RH. Specifically, population 1 is considered as protons in polymer chains; population 2 and 3 are mainly contributed by water molecules; population 4 and 5 are attributed to protons in IL. Herein, the appearance of population 5 on the diagonal line could be related to a small amount of IL leakage at 90% RH. Moreover, the existence of two water species at high RH indicates that additional water molecules are weakly bonded to polymer chains and act as a plasticizer to soften the ionogel, which is in accordance with the modulus change under different RH.

2.3. H-Bonding Evolution During Phase Separation

H-bonding structures responsible for the water-induced phase separation of the ionogel are further validated by infrared spectroscopy. **Figures** 4a and S13 (Supporting Information) displays the FTIR spectra of the ionogel in the dry state and equilibrated at varied RH. The increased intensity in 3700–3200 cm^{-1} region with higher RH indicates that more water molecules are absorbed into the ionogel. In addition, the Amide I region, mainly contributed by C═O stretching vibration, exhibits an obvious shift to lower wavenumber after hydration, suggesting a H-bonding strengthening process for C═O groups in PNIPAM. For

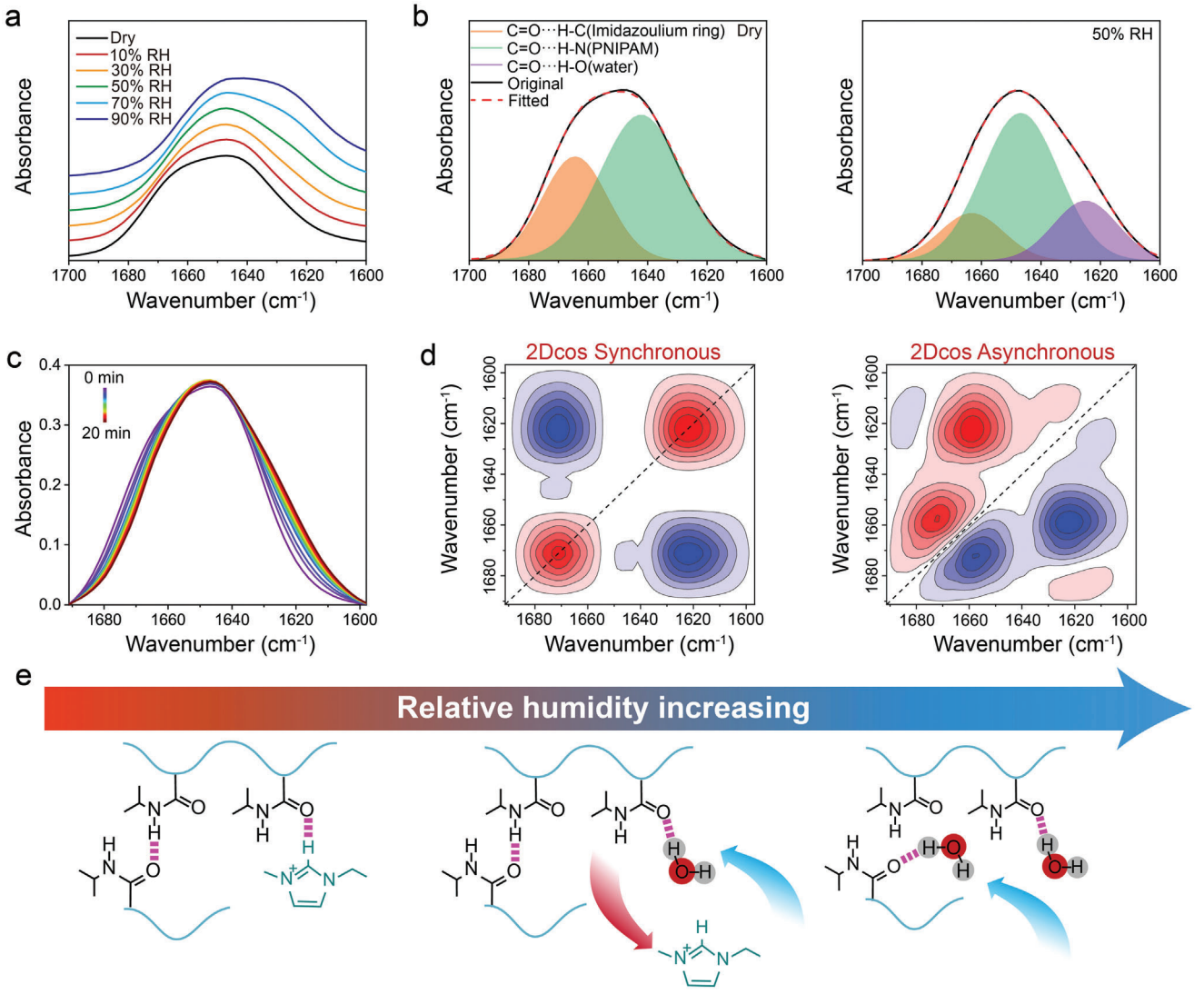

Figure 4. Molecular interactions in the PNIPAM/[EMIM][TFSI] ionogel: a) FTIR spectra of ionogel in the dry state and equilibrated at different RH. b) Curve fitted Amide I region in the dry state and equilibrated at 50% RH. c) Time-dependent FTIR spectra during moisture absorption at ≈50% RH. d) 2Dcos synchronous and asynchronous spectra generated from (c). e) Schematic illustration of H-bonding transformation during dynamic hydration of the ionogel.

better demonstration, the Amide I region is fitted with Gaussian curve, as shown in Figure 4b and Figure S14 (Supporting Information). In the dry ionogel, C=O groups mainly form H-bonds with C—H groups in the imidazolium ring and NH groups in PNIPAM and the delicate balance between C=O...H—C (imidazolium ring)[14b,17] and C=O...H—N (PNIPAM)[18] H-bonding structures affords a homogeneous phase of the ionogel. After absorbing water, which holds a strong capability to participate in H-bonding, C=O would preferably form H-bonds with water, thus breaking the H-bonding structure of C=O...H—C (imidazolium ring). Consequently, the balance between polymer–polymer and polymer-IL interactions is interrupted, leading to the occurrence of phase separation. Since [EMIM][TFSI] is hydrophobic and incompatible with water, the absorbed water molecules mainly locate in the polymer-rich phase. After further increasing the RH, the portion of C=O...H—O (water)[19] H-bonding continues increasing, which would interrupt the C=O...H—N (PNIPAM) H-bonding and cause plasticizing effect in the polymer-rich phase, thus deteriorating the stiffness of the ionogel. Herein, it should be noted that, in addition to C=O...H—O (water) H-bonding structures, water could also form H-bonds with N—H groups in PNIPAM (Figure S15, Supporting Information). From this point of view, the stiffness variation of the ionogel during hydration is closely related to the H-bonding structures in the system.

Furthermore, we in situ monitor the molecular interaction variation in the ionogel by collecting time-dependent FTIR spectra during water absorption at ≈50% RH. As shown in Figure 4c, the Amide I region exhibits a bidirectional change with intensity decreasing at higher wavenumbers while increasing at lower wavenumbers with hydration, revealing the transformation of C=O...H—C (imidazolium ring) into C=O...H—O (water) H-bonds. 2D correlation spectroscopy (2Dcos) is employed

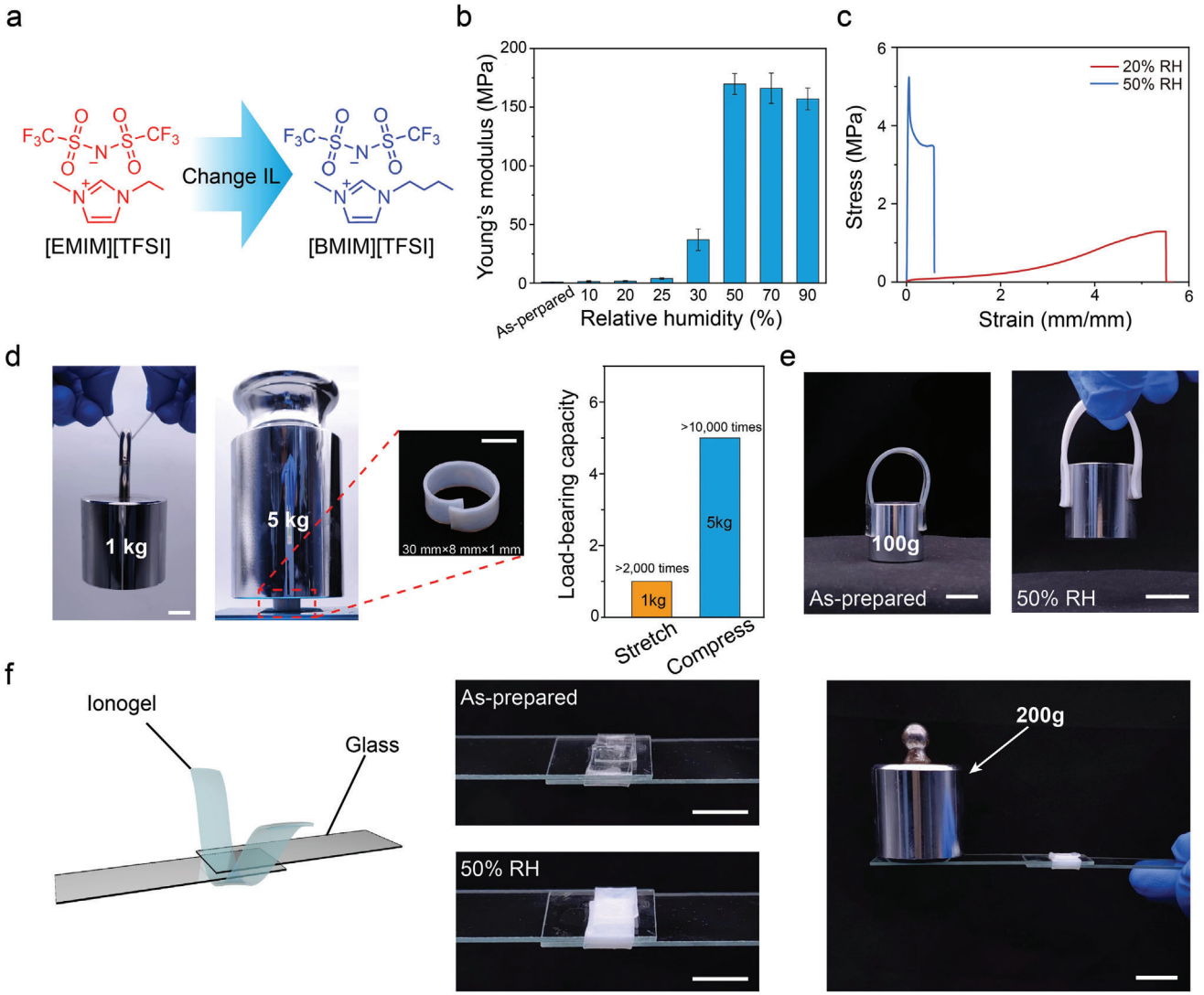

Figure 5. a) Chemical structures of [EMIM][TFSI] and [BMIM][TFSI]. b) Young's modulus of PNIPAM/[BMIM][TFSI] ionogel at varied RH. c) Tensile stress–strain curves of PNIPAM/[BMIM][TFSI] ionogel at 20% and 50% RH. d) Photographs showing the load-bearing capability and shape reconfigurability d), soft-to-stiff transitional contact e) of the PNIPAM/[EMIM][TFSI] ionogel. f) Demonstration of PNIPAM/[EMIM][TFSI] ionogel as "smart rope". Scale bars in the figures are 1 cm.

to investigate the dynamic change of C=O groups during water absorption (Figure 4d). In the 2Dcos asynchronous map, three subtle bands at 1672, 1657, and 1622 cm^{-1} have been identified, which could be assigned to C=O groups H-bonded with C—H (imidazolium ring), N—H (PNIPAM) and OH (water) from high to low wavenumbers, respectively. On the basis of Noda's rule,[20] the change sequency of all the three bands during hydration follows ("→" means "prior to"): 1622 → 1672 → 1657 cm^{-1}, that is, ν(C=O) (H-bonded with O—H in water) → ν(C=O) (H-bonded with C—H in imidazolium ring) → ν(C=O) (H-bonded with N—H in PNIPAM), emphasizing the dominant role of polymer–water H-bonding in the water-induced phase separation. In addition, it is inferred that the presence of water would break the polymer-IL and polymer-polymer H-bonding in sequence. For clarity, the H-bonding transformation during dynamic hydration of the ionogel is illustrated in Figure 4e.

2.4. Modulation and Applications of the Humidity-Induced Stiffening of the Ionogel

The PNIPAM/[EMIM][TFSI] binary ionogel exhibits an obvious stiffening even after exposure to relatively low RH, leading to the difficulty in controlling such a stiffness-switching behavior. It is speculated that the presence of more hydrophobic IL in the ionogel might prevent water absorption in some extent, which provides a clue to modulate the humidity-responsive property of the ionogel. Then, we use 1-butyl-3-methylimidazolium bis(trifluoromethylsulfonyl) imide ([BMIM][TFSI]) (**Figure 5a**), instead of [EMIM][TFSI], to construct the binary ionogel and examine the water-induced stiffening behavior. As shown in Figure S16 (Supporting Information), the PNIPAM/[BMIM][TFSI] ionogel exhibits a phase separation with apparent stiffening after moisture absorption at 50% RH. Unlike PNIPAM/[EMIM][TFSI]

ionogel, the PNIPAM/[BMIM][TFSI] ionogel remains soft and apparent under 20% RH while becomes opaque with dramatically increased E at 30% RH (Figure 5b,c; Figure S17, Supporting Information), demonstrating a delayed stiffening with RH increasing.

Holding dramatic humidity-responsive stiffness-variation, the PNIPAM/[EMIM][TFSI] ionogel demonstrates original capabilities for a wide range of applications. Major advantages of the ionogel toward application are: (1) shape adaptability and shape reconfigurability; (2) spontaneous stiffening upon exposure to air. The ionogel strip can be manually configured into diverse structures for load-bearing and support a weight over 10, 000 times its own weight (Figure 5d). The as-prepared ionogel is adaptable to curved objects with increased contact area and subsequent humidity-induced stiffening could lock the interface for adhesion (Figure 5e). Furthermore, the ionogel can be used as "smart rope", which is soft for configuration in the as-prepared dry state and becomes stiff after moisture absorption for fixation (Figure 5f).

3. Conclusion

In this work, we report a simple binary ionogel, composed of PNIPAM and IL, with dramatic water-induced stiffening enabled by H-bonding competition mediated phase separation, demonstrating a dynamic solution for simultaneous shape adaptability and load-bearing capability. The binary ionogel could transform from a transparent and soft state into an opaque and highly stiff one after moisture absorption. Our detailed analyzes reveal that the stiffness switching of the ionogel under hydration is closely related to the H-bonding structures, where absorbed water molecules in the ionogel could compete in H-bonding with polymer chains and interrupt the delicate balance between polymer–polymer and polymer-IL H-bonding, leading to phase separation structures with boosted modulus. Meanwhile, additional water molecules would cause plasticizing effect in the polymer-rich phase and deteriorate the stiffness of the ionogel. Having understand the stiffening mechanism from the molecular level, we anticipate that this H-bonding competition concept could be extended to design other stiffness switching polymer materials for various load-bearing scenarios.

Supporting Information

Supporting Information is available from the Wiley Online Library or from the author.

Acknowledgements

The authors gratefully acknowledge the financial support of the Fundamental Research Funds for the Central Universities (No. 2232022A-08) and the Research Foundation of National Innovation Center of Advanced Dyeing & Finishing Technology (No. 2022GCJJ07).

Conflict of Interest

The authors declare no conflict of interest.

Data Availability Statement

The data that support the findings of this study are available from the corresponding author upon reasonable request.

Keywords

hydrogen bond, ionogel, phase separation, stiffness-switch, water-responsive

[1] a) D. Nepal, S. Kang, K. M. Adstedt, K. Kanhaiya, M. R. Bockstaller, L. C. Brinson, M. J. Buehler, P. V. Coveney, K. Dayal, J. A. El-Awady, L. C. Henderson, D. L. Kaplan, S. Keten, N. A. Kotov, G. C. Schatz, S. Vignolini, F. Vollrath, Y. Wang, B. I. Yakobson, V. V. Tsukruk, H. Heinz, *Nat. Mater.* **2023**, *22*, 18; b) F. Libonati, A. E. Vellwock, F. Ielmini, D. Abliz, G. Ziegmann, L. Vergani, *Sci. Rep.* **2019**, *9*, 3142.

[2] J. R. Capadona, K. Shanmuganathan, D. J. Tyler, S. J. Rowan, C. Weder, *Science* **2008**, *319*, 1370.

[3] a) S. M. Mirvakili, I. W. Hunter, *Adv. Mater.* **2018**, *30*, 1704407; b) J. Wang, D. Gao, P. S. Lee, *Adv. Mater.* **2021**, *33*, 2003088; c) L. Zhang, S. Wang, Z. Wang, Z. Liu, X. Xu, H. Liu, D. Wang, Z. Tian, *ACS Nano* **2023**, *17*, 13948; d) C. Ni, D. Chen, Y. Yin, X. Wen, X. Chen, C. Yang, G. Chen, Z. Sun, J. Wen, Y. Jiao, C. Wang, N. Wang, X. Kong, S. Deng, Y. Shen, R. Xiao, X. Jin, J. Li, X. Kong, Q. Zhao, T. Xie, *Nature* **2023**, *622*, 748; e) F. Wu, Y. Pang, J. Liu, *Nat. Commun.* **2020**, *11*, 4502; f) L. Zhang, H. Yan, J. Zhou, Z. Zhao, J. Huang, L. Chen, Y. Ru, M. Liu, *Adv. Mater.* **2023**, *35*, 2202193; g) H. Fan, J. Wang, J. P. Gong, *Adv. Funct. Mater.* **2021**, *31*, 2009334.

[4] a) L. Chen, C. Zhao, J. Huang, J. Zhou, M. Liu, *Nat. Commun.* **2022**, *13*, 6821; b) X. Zhang, C. Zhu, B. Xu, L. Qin, J. Wei, Y. Yu, *ACS Appl. Mater. Interfaces* **2019**, *11*, 46212; c) F. Yang, A. Cholewinski, L. Yu, G. Rivers, B. Zhao, *Nat. Mater.* **2019**, *18*, 874.

[5] a) H. Wan, B. Wu, L. Hou, P. Wu, *Adv. Mater.* **2024**, *36*, 2307290; b) J. Huang, Y. Jiang, Q. Chen, H. Xie, S. Zhou, *Nat. Commun.* **2023**, *14*, 7131; c) Y. Fang, Z. Bai, L. Yang, Q. Liu, W. Xu, J. Wei, K. Yang, Q. Wang, J. Cui, *Adv. Funct. Mater.* **2024**, *34*, 2314353; d) H. Feng, Y. Sheng, G. Chen, B. Jin, Z. Fang, B. Yang, X. Zhou, W. Wu, T. Xie, N. Zheng, *CCS Chem.* **2024**, *6*, 682.

[6] a) M. Wang, P. Zhang, M. Shamsi, J. L. Thelen, W. Qian, V. K. Truong, J. Ma, J. Hu, M. D. Dickey, *Nat. Mater.* **2022**, *21*, 359; b) J. Wu, Z. Zhang, Z. Wu, D. Liu, X. Yang, Y. Wang, X. Jia, X. Xu, P. Jiang, X. Wang, *Adv. Funct. Mater.* **2023**, *33*, 2210395; c) T. Nonoyama, Y. W. Lee, K. Ota, K. Fujioka, W. Hong, J. P. Gong, *Adv. Mater.* **2020**, *32*, 1905878; d) J. Wu, B. Wu, J. Xiong, S. Sun, P. Wu, *Angew. Chem., Int. Ed.* **2022**, *61*, e202204960.

[7] a) Z. Xu, M. Wu, W. Gao, H. Bai, *Sci. Adv.* **2022**, *8*, eabo0946; b) K. Gong, L. Hou, P. Wu, *Adv. Mater.* **2022**, *34*, 2201065.

[8] a) Z. Tai, J. Wei, J. Zhou, Y. Liao, C. Wu, Y. Shang, B. Wang, Q. Wang, *Nat. Commun.* **2020**, *11*, 1843; b) T. Igarashi, M. Hoshi, K. Nakamura, T. Kaharu, K.-I. Murata, *J. Phys. Chem.* **2020**, *124*, 4196.

[9] a) J. Sun, H. He, K. Zhao, W. Cheng, Y. Li, P. Zhang, S. Wan, Y. Liu, M. Wang, M. Li, Z. Wei, B. Li, Y. Zhang, C. Li, Y. Sun, J. Shen, J. Li, F. Wang, C. Ma, Y. Tian, J. Su, D. Chen, C. Fan, H. Zhang, K. Liu, *Nat. Commun.* **2023**, *14*, 5348; b) K. Yu, Z. Feng, H. Du, K. H. Lee, K. Li, Y. Zhang, S. F. Masri, Q. Wang, *PNAS Nexus* **2022**, *1*, pgac139.

[10] a) M. Li, H. Lu, M. Pi, H. Zhou, Y. Wang, B. Yan, W. Cui, R. Ran, *Adv. Sci.* **2023**, *10*, 2304780; b) S. Ishikawa, Y. Iwanaga, T. Uneyama, X. Li,

H. Hojo, I. Fujinaga, T. Katashima, T. Saito, Y. Okada, U.-i. Chung, N. Sakumichi, T. Sakai, *Nat. Mater.* **2023**, *22*, 1564.
[11] J. Xu, D. A. Bohnsack, M. E. Mackay, K. L. Wooley, *J. Am. Chem. Soc.* **2007**, *129*, 506.
[12] W. Liu, A. Wang, R. Yang, H. Wu, S. Shao, J. Chen, Y. Ma, Z. Li, Y. Wang, X. He, J. Li, H. Tan, Q. Fu, *Adv. Mater.* **2022**, *34*, 2201914.
[13] X. Ming, L. Yao, H. Zhu, Q. Zhang, S. Zhu, *Adv. Funct. Mater.* **2022**, *32*, 2109850.
[14] a) S. De Santis, C. L. Mesa, G. Masci, *Polymer* **2017**, *120*, 52; b) C. Wang, P. Li, S. Zhang, G. Zhang, S. Tan, Y. Wu, M. Watanabe, *Macromolecules* **2020**, *53*, 4901.
[15] K. Morishima, X. Li, K. Oshima, Y. Mitsukami, M. Shibayama, *J. Chem. Phys.* **2018**, *149*, 163301.
[16] a) Y. Shi, B. Wu, S. Sun, P. Wu, *Adv. Mater.* **2024**, *36*, 2310576; b) H. Ye, B. Wu, S. Sun, P. Wu, *Nat. Commun.* **2024**, *15*, 885.
[17] Z. Wang, P. Wu, *J. Phys. Chem. B* **2011**, *115*, 10604.
[18] a) B. Sun, Y. Lin, P. Wu, H. W. Siesler, *Macromolecules* **2008**, *41*, 1512; b) H. Cheng, L. Shen, C. Wu, *Macromolecules* **2006**, *39*, 2325.
[19] Y. Maeda, T. Higuchi, I. Ikeda, *Langmuir* **2000**, *16*, 7503.
[20] a) I. Noda, *Appl. Spectrosc.* **1993**, *47*, 1329; b) W. Zhang, B. Wu, S. Sun, P. Wu, *Nat. Commun.* **2021**, *12*, 4082.